Journal of Metals, Materials and Minerals, Vol. 33, No. 2, pp. 38-52, 2023

Effect of nano CdO-ZnO content on structural, thermal, optical, mechanical and electrical properties of epoxy composites

Chaitra SRIKANTH[1,*], and Gattumane Motappa MADHU[1,2]

[1] *Department of Chemical Engineering, M S Ramaiah Institute of Technology, MSR Nagar, Bangalore, Karnataka, 560054 India*
[2] *Centre for Advanced Materials Technology, M S Ramaiah Institute of Technology, MSR Nagar, Bangalore, Karnataka, 560054 India*

***Corresponding author e-mail:** chaitra.srikanth@msrit.edu

Received date:
5 January 2023
Revised date
11 April 2023
Accepted date:
18 April 2023

Keywords:
CdO-ZnO;
Epoxy;
Tensile properties;
Flexural properties;
Compressive properties

Abstract

Cadmium oxide doped zinc oxide nanoparticles were synthesized by solution combustion technique. CdO-ZnO nanoparticles were reinforced into epoxy by ultrasonication technique. CdO-ZnO nanoparticles are well known semiconducting materials which are found to exhibit excellent semiconducting behavior even at high frequencies. Hence it was introduced into epoxy to study the semiconducting nature of CdO-ZnO/epoxy composites. The polymer composites exhibited interesting phenomenon such as minimum heat losses at high frequencies indicating semi-conducting behaviour of the composites. The polymer composite was also analysed for its structural, thermal, optical and mechanical properties. The enhanced interaction of CdO-ZnO nanoparticles with epoxy has resulted in superior UV-shielding effeciency and mechanical properties. This paper mainly focusses upon the synthesis and development of CdO-ZnO/epoxy composites, the design and optimization of CdO-ZnO compositions, the mechanical toughening and failure mechanism, transport mechanism of charge carriers, conductivity relaxation, ionic polarization and prospects of CdO-ZnO/epoxy composites in various fields.

1. Introduction

Nanotechnology is an evolving field of science due to the extensive investigation on the nanomaterials, especially polymer composites. Polymer composites involve two major components, one is matrix and the other reinforcement. The properties of the matrix are enhanced by the reinforcing materials which are generally the nanomaterials. Thermosetting polymers such as epoxy are used as matrix materials since they possess good temperature resistance and low creep properties. Epoxies exhibit high degree of cross-linking in the polymer networks resulting into a brittle material. Most of the undesirable nature of the epoxies can be ruled out by reinforcing with nanomaterials. The incorporation of these nanoparticles as reinforcing materials have contributed to increase in toughness, modulus, strength and improved fracture properties. Epoxy based polymer composites are trending materials due to their incredibly high performance at high temperatures, excellent mechanical properties as well as their thermal behaviour [1].

The size of a nanomaterial plays a significant role in the synthesis of the composite [2]. When a material of size ranging in few microns such as fibre glass, aramid etc. are reinforced in a matrix, it significantly improved the load bearing capacity of the composite, its strength and stiffness, but the material fails to offer good impact resistance [2,3]. One way to overcome this problem is to reduce the size of the material from microns to a few nanometers. Designing materials on a nanometer level has its own advantages such as high aspect ratio and high surface area [4]. Wetzel *et al*. [5] studied the effect of reinforcing particles in the size of microns and nanoparticles and compared the results. They also compared the synergistic effect between micro particles and nanoparticles. The reason behind choosing nanoparticles as filler materials was due to the rapid increase in the number of particles for a given volume which induce excellent mechanical properties by completely transforming the nature of the polymer composite itself. When a particle of size 1 μm is replaced with a particle of size 10 nm it is profoundly increasing the absolute number of particles by a factor of 100 for a given volume. This would significantly change the properties of the composite material from the bulk to nanodomain due to the interfacial interactions between the polymer matrix and the nanofiller resulting in an entirely new class of materials for our beneficial endeavour [6].

Uniform and homogeneous distribution of the nanoparticles in the epoxy matrix plays a vital role in making a polymer composite unique and enhancing its overall mechanical properties. Many researchers [7-11] have reported that low concentrations of nano filler such as 1 wt% to 5 wt% there is a significant improvement in the mechanical properties. There are two methods by which nanoparticles can be uniformly distributed into epoxy matrix. One is by chemical methods such as graft polymerization with/without a coupling agent [12]. The other method is by applying physical forces such as shear force [13] i.e., by mixing using a rotating disc at a high speed. Another means of uniform and homogeneous distribution of nanofiller in epoxy matrix is by using high frequency sound waves generated by an ultrasonicator [14,15].

Some researchers reported that, ZnO was used as a nanofiller in epoxy and was found to improve the surface damage of the resin

under multiscratching conditions after viscoelastic recovery. The researchers found that addition of ZnO nanoparticles increased the stiffness of epoxy [16]. Effect of ZnO concentration on mechanical properties of epoxy was investigated and reported by Ding *et al*. [17]. They found that flexural strength and tensile properties such as ultimate tensile strength, tensile modulus, energy at break were enhanced significantly. Improved crack resistance was also observed upto 5 wt% of ZnO in epoxy, further increase in filler content led to a decline in mechanical properties. In our previous research work, we have reinforced CdO-ZnO nanoparticles in PVA and studied its structural, electrical and mechanical properties [18]. Currently, our aim is to reinforce CdO-ZnO nanoparticles into epoxy matrix and report its influence on structural, thermal, optical, mechanical and electrical properties of nano CdO-ZnO/epoxy composites.

The aim of the present work is to incorporate varying concentrations of CdO-ZnO nanofiller into the epoxy matrix by ultrasonication technique. Epoxy was doped with 0 wt% to 2.5 wt% CdO-ZnO nanoparticles to study the influence of filler concentration on structural properties of nano CdO-ZnO/epoxy composites using Scanning Electron Microscope (SEM), X-Ray Diffractometer (XRD) and Fourier Transform Infra-Red Spectroscopy (FTIR spectra). Optical properties were analysed using UV-Visible Spectroscopy (UV-Vis spectra). All epoxy composites exhibited excellent UV-shielding capacity with increase in nano CdO-ZnO content. Thermal properties such as Differential Scanning Calorimetry (DSC), Thermogravimetric Analysis (TGA) and Derivative Thermogravimetry (DTG) were performed to analyse the thermal degradation and thermal stability of nano CdO-ZnO/epoxy composites. Electrical properties such as impedance spectroscopy, dielectric permittivity, electrical modulus and electrical conductivity were carried out to study the semiconducting behaviour at high frequencies. The semiconducting behaviour of polymer composites enhanced with increase in filler content. Nano CdO-ZnO epoxy composites were assessed for its mechanical properties such as compression properties, tensile properties and flexural properties using Zwick Ultimate Tensile Testing Machine (UTM). Improvement in mechanical properties were observed upto 1 wt% CdO-ZnO/epoxy and later declined with increase in filler content. The failure mechanism of epoxy composites at high filler content is also discussed in detail. These high performance epoxy composites may be useful in finding industrial applications that demand semiconducting epoxy composites that exhibit enhance UV-shielding capacity with superior mechanical properties along with good thermal stability in the field of adhesives, electronics and aerospace.

2. Materials and methods

2.1 Chemicals

Epoxy resin used for our experimental purpose was Lapox L-12 resin, it is a Bisphenol-A based resin along with a polyamine K-6 hardener which was used as a curing agent.

2.2 Fabrication of CdO-ZnO nano-filler in epoxy

Epoxy of known quantity was taken and sonicated for 40 min in an ultrasonicator (200 W), the temperature of the epoxy began to rise upto 70°C and the mixture was allowed cool for few minutes until it reached room temperature and then it was mixed with the hardener and casted onto a mould. The mixture was allowed to dry at room temperature for 48 h. A standard composition of 90% resin and 10% hardener by volume was mixed to obtain plain epoxy. Similar procedure was carried out for polymer composites doped with CdO-ZnO. Initially, the epoxy was mixed with a known quantity of nanopowder and sonicated for 40 min followed by cooling and mixing with hardener and casting the entire mixture in a mould. This procedure was carried out for different weight percentages (wt%) of nanopowder in epoxy such as 1, 1.5, 2, and 2.5 wt%. The resultant epoxy and epoxy composites obtained after drying were found to be free from air bubbles. Thickness of plain epoxy was found to be 2.62 mm, whereas for epoxy composites it was found to be ranging from 2.65 mm to 2.82 mm. Thickness measurements were made using LCD digital Vernier callipers.

2.3 Characterization techniques and measurements

Characterization of CdO-ZnO nanoparticles synthesized by solution combustion method is already reported in our previous paper [18]. X-ray diffraction (XRD) measurements were performed using Bruker D8 Advance X-ray diffractometer (Cu kα; λ=1.54 Å) at room temperature with 2θ ranging from 10° to 80° and a step size of 0.02°. The surface morphology of the as-synthesised nano powders and the tensile fractured specimens were studied using a Field Emission Scanning electron microscope (FESEM)-Gemini ultra55 (Zeiss) under an accelerating voltage of 5 kV. Energy dispersive X-ray spectroscopy (EDX) was employed using Oxford INCA EDS detector attached to the FESEM. All the samples were Au-sputtered before the measurements. UV-VIS diffuse reflectance spectroscopy (DRS) measurements were acquired using Perkin-Elmer Lambda 365 in the wavelength range of 200 nm to 1100 nm. The spectral data was recorded in terms of %transmittance with a spectral bandwidth of 5 nm. Bruker Alpha Fourier transform infrared spectrometer (FTIR) was used to analyse the samples in transmittance mode in the spectral range of 4000 cm^{-1} to 500 cm^{-1} with a resolution of 4 cm^{-1}. Raman spectrometer LabRAM HR (Horiba Jobin Yvon, France) was employed for recording the Raman spectra with an excitation wavelength of 532 nm. Thermal properties such as Differential scanning calorimetry (DSC), Thermogravimetric analysis (TGA) and Derivative thermogravimetry (DTG) of epoxy composites were investigated using a simultaneous thermal analyser (STA)-NETZSCH STA 449 F1 Jupiter with a temperature range of 40°C to 800°C. The ramp rate was fixed at 10°C·min^{-1} with continuous purging of dry N_2 gas to the furnace. All the mechanical properties such as Tensile, compressive and flexural were tested using Zwick Universal Tensile Testing Machine (UTM). Tensile properties testing was performed as per ASTM D638 standard testing procedure. The crosshead speed was 10 mm·min^{-1}. Compression properties testing was performed as per ASTM D695 standard testing procedure. The testing speed was 2 mm·min^{-1}. Flexural properties testing was performed as per ASTM D790 standard testing procedure. The preload speed was 5 mm·min^{-1}. Three samples for each composition of the composite was taken and tested. The average values are reported. Frequency-dependent impedance and dielectric properties were measured using Agilent 4294A Impedance Analyzer. Before the measurements, the samples were coated with a thin layer of Ag conductive paste and allowed to dry at room temperature.

3. Results and discussion

3.1 SEM and EDX

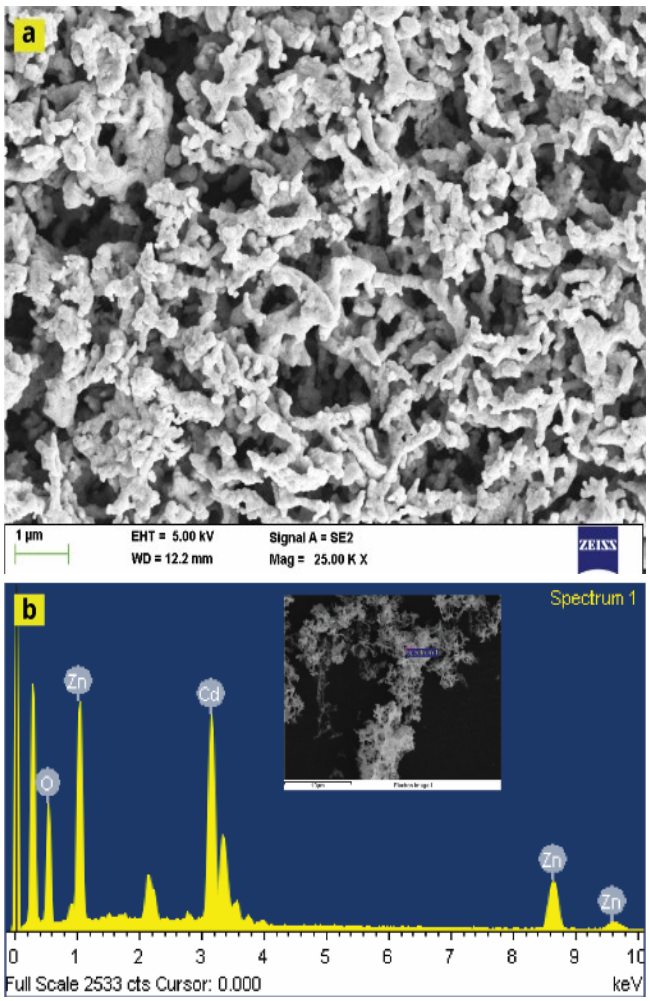

Figure 1. (a) SEM micrograph of CdO-ZnO nanoparticles and (b) EDX spectrum of CdO-ZnO nanoparticles. Inset shows the position selected for EDX scan.

Figure 1 shows the SEM image and EDX spectra of CdO-ZnO nanoparticles. The micrograph (Figure 1(a)) depicts a linear grain-like structure of the nanoparticles with high degree of aggregation. The micrograph also reveals that the structure is porous.

The size of the nanoparticle was found to be ~50 nm, whereas the agglomerated particle size was found to be ~150 nm. In addition, the EDX spectrum (Figure 1(b).) show strong peaks at ~0.5, 1.0, and 3.0 keV corresponding to oxygen (76 at%), zinc (12.8 at%), and cadmium (10.9 at%), respectively.

3.2 XRD

CdO-ZnO nanopowder prepared by solution combustion method was characterized for XRD and the results are shown in Figure 2. Sharp prominent peaks were observed which indicated that the nanopowder is crystalline in nature. The results showed that CdO was found to exist in cubic halite (monteponite) structure with lattice constant a = 4.695Å. Whereas, ZnO was found to exhibit hexagonal wurtzite (zincite) structure with lattice constants a = 3.250Å and c = 5.207Å. Eleven dominant peaks were observed at different 2θ positions. The diffraction peaks were observed for CdO at 2θ values = 33.01°, 38.31°, 55.29°, 65.93°, 69.26° and 82.02° which are indexed with (111), (200), (220), (311), (222) and (400) respectively. ZnO diffraction peaks were observed at 2θ values = 31.76°, 34.41°, 36.25°, 47.53°, 56.58°, 62.85° and 66.36° which are indexed with (100), (002), (101), (102), (110), (103) and (200) respectively. The diffraction peak positions of CdO matched well with ICDD No. 005-0640 and ZnO with ICDD No. 036-1451. The diffractogram's peak positions, h,k,l values, plane positions and ICDD card numbers matched with the literature values as well [18]. Debye-Scherrer formula was used to calculate the size of the crystallite, as shown in Equation (1) [18]:

$$t = 0.9\lambda/\beta\text{Cos}\theta \quad (1)$$

where: λ = wavelength of the x-rays used (1.5406Å for Cukα source),
β = full width at half maximum,
θ = angle of diffraction.

The average calculated particle size was found to be = 54.133 nm

XRD pattern of plain epoxy and epoxy doped with varying concentrations of CdO-ZnO (0.5 wt% to 2.5 wt%) are shown in Figure 3, it is cleary evident that epoxy doesn't exhibit sharp, crystalline peaks and it is an amorphous polymer [19]. Increase in filler content has led to increase in sharp, prominent, crystalline peaks indicating increase in crystallinity of polymer composites. The intensity of the diffraction peaks also increased with increase in CdO-ZnO content in epoxy/CdO-ZnO composites with the same peak positions as obtained for the pure CdO-ZnO nanopowder. The broad peak obtained at 2θ=20° in all the XRD patterns in Figure 3 corresponds to the epoxy peak [20]. All the diffraction peaks increased linearly with increase in nano filler content indicate that there was no great loss of CdO-ZnO content in epoxy during the fabrication process of all the samples at any given weight percentage. Hence, all the polymer composites reflect the exact weight content.

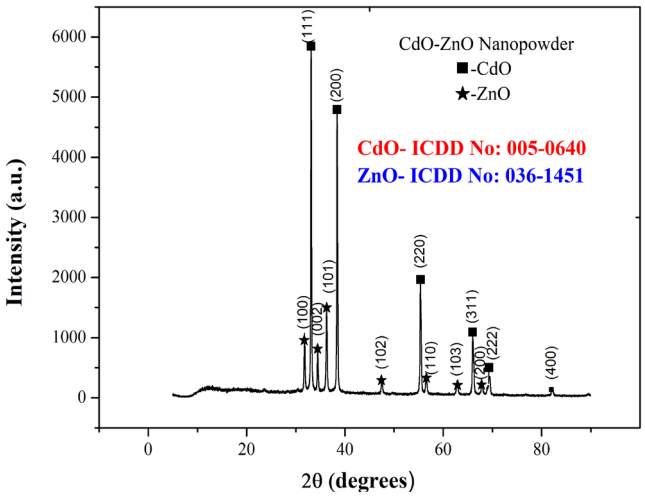

Figure 2. XRD data of CdO-ZnO nanopowder.

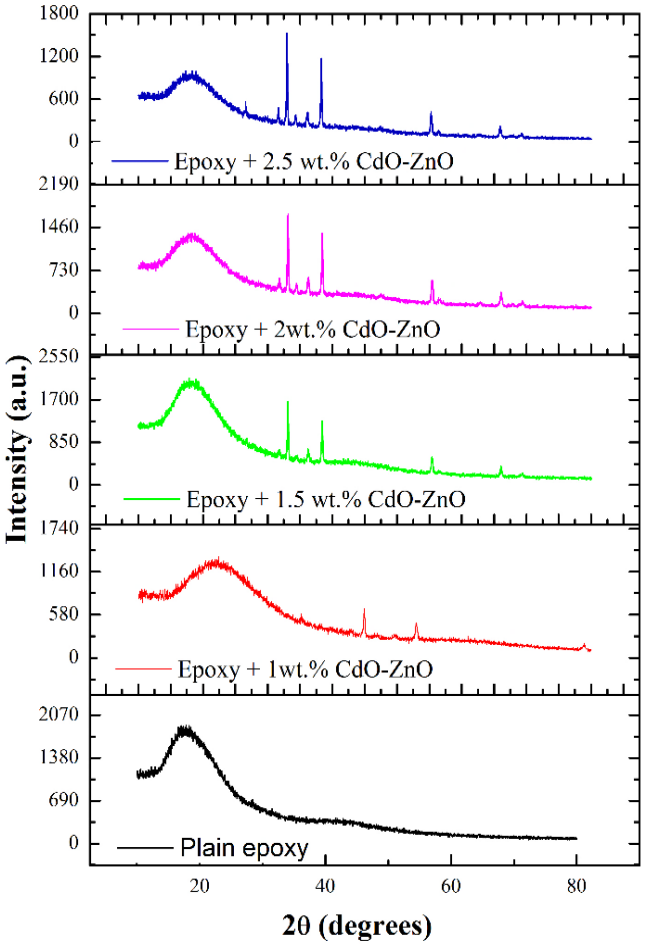

Figure 3. XRD data of epoxy/CdO-ZnO composites.

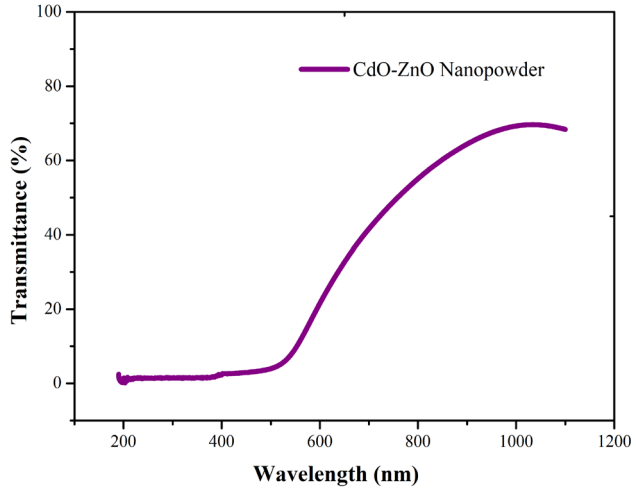

Figure 4. UV-Vis spectra for CdO-ZnO nanopowder.

3.3 UV-Vis spectra

Figure 4 shows the UV-Vis spectra of CdO-ZnO nanopowder. It is clearly evident that, CdO-ZnO nanopowder exhibited very low transmittance (8 % to ~100 %) of UV light in the wavelength range 200 nm to 550 nm, which indicates excellent UV-shielding capacity of the nanopowder at low wavelength range. This might be due to calcination of nanopowder at high temperature (600°C) leading to enhanced UV shielding capacity [21]. With increase in wavelength from 550 nm to 1100 nm an exponential increase in transmittance of UV light was observed.

UV-Vis Spectra for plain epoxy and epoxy loaded with varying concentrations of CdO-ZnO composites in the region of 200 nm to 1100 nm are shown in Figure 5. It is observed that transmittance of UV light decreased with increase in nano filler concentration in the epoxy composites [21]. All the epoxy composites exhibited ~100% UV shielding efficiency upto 600 nm. Whereas epoxy with 2.5 wt% CdO-ZnO exhibited ~100% UV shielding efficiency upto 800 nm, only a slight decrease in UV shielding efficiency was observed with further increase in wavelength upto 1100 nm. However, increase in CdO-ZnO concentration in epoxy reduced the visible light transparency of the epoxy composites. This is because, CdO-ZnO nanoparticles are opaque particles. After ultrasonication of CdO-ZnO nanoparticles with epoxy, the entire composite is transformed into an opaque polymer composite. Hence reducing the visible light transparency of polymer composites.

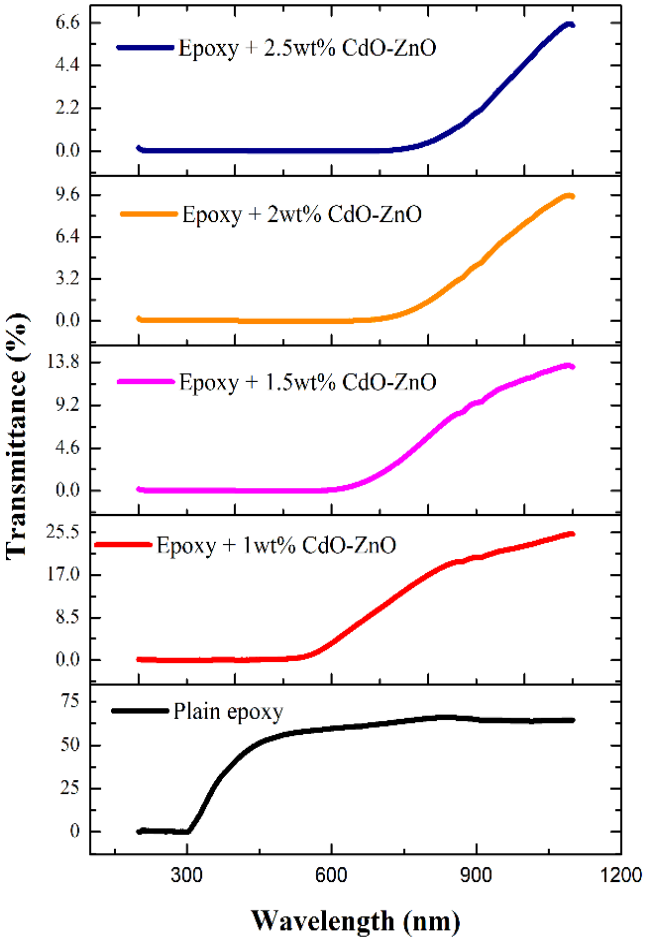

Figure 5. UV-Vis spectra of epoxy/CdO-ZnO composites.

Table 1. Effect of CdO-ZnO addition on thermal behaviour of epoxy composites.

CdO-ZnO content (wt%)	T_g (ºC)	$T_{10\%}$ (ºC)	$T_{50\%}$ (ºC)	T_{max} (ºC)	dW/dT_{max} (ºC)	% residual $mass_{800}$
0.0	73.91	345.50	379.64	368.05	-13.71	8.33
1.0	69.63	332.89	396.86	397.58	-16.40	12.72
1.5	72.19	275.78	390.55	390.57	-15.39	12.92
2.0	75.18	323.26	390.91	390.62	-17.01	14.68
2.5	74.71	328.25	389.88	387.20	-17.50	15.28

3.4 DSC-TGA-DTG

The glass transition temperature (T_g) values of composites (Table 1, Figure 6(a)) show slight improvement with increasing nanofiller content. The highest T_g was shown by epoxy/2.5 wt% CdO-ZnO (74.71°C) and the lowest T_g was exhibited by epoxy/1.0 wt% CdO-ZnO (69.13°C). However, plain epoxy showed a T_g value of 73.91°C.

This deviation from the expected trend indicates that the dispersion of nanoparticles inside the matrix is non-ideal. The degree of dispersion of nano fillers inside the base matrix is crucial as it interferes with the transitional behaviour of the polymer due to the introduction of secondary phase agglomerations [22]. This anomalous interaction has been reported by a few researchers in the literature [22-25]. The agglomeration of the fillers in the matrix also induces free volume between the filler-resin interface and ultimately lowers the cross-linking density [19]. This in turn causes the T_g to fluctuate. The thermal weight loss behaviour of epoxy composites also displays the same trend.

Figure 6(b). shows the TGA and its first derivative of the fabricated composites and Table 1 lists a few parameters that are important for evaluating the thermal stability of these composites such as: $T_{10\%}$ gives the temperature after a weight loss of 10%, which is sometimes considered as the onset of degradation (T_{onset}). Similarly, $T_{50\%}$ gives the temperature after a weight loss of 50% and T_{max} is the temperature at maximum decomposition (extracted from the 1st derivative). Finally, % char residue is the weight % of the material left at the end of the experiment. As observed from the graph, the introduction of nano CdO-ZnO to the amine-modified epoxy matrix has unexpectedly reduced the onset of degradation temperature. The $T_{10\%}$ of plain epoxy is 345.5°C, whereas the $T_{10\%}$ for the composites with 1.0, 1.5, 2.0 and 2.5 wt% of CdO-ZnO are 332.89, 275.78, 323.26 and 328.25°C respectively. This unusual trend has been reported in some papers. For instance, Chee and Jawaid [26] observed a decrease in the T_{onset} values for epoxy incorporated with organically modified montmorillonite (OMMT) composites. The authors argued that the presence of organic surface modifiers and complex ammonium salts functionalized on the surface of clay particles might have catalysed the degradation process. Nguyen *et al.* [23] reasoned that the first step of degradation generally occurs due to the evaporation of (interstitial) water molecules from the oxy-propylene ring and other volatile compounds such as the hardener. On the other hand, it is also possible that aggregations induced due to the nanoparticles might create free volume and irregular pores inside the matrix and enhance the degradation process.

From Figure 6(c) it can be observed that that the fabricated composites exhibited multi-step degradation [27]. Nguyen *et al.* reasoned that the first step of degradation generally occurs due to the evaporation of water molecules from the oxy-propylene ring and other volatile compounds such as the amine-hardener. On the other hand, it is also possible that aggregations induced due to the nanoparticles might create free volume and irregular pores inside the matrix and enhance the degradation process. The second major degradation step occurs due to the breakdown of high molecular weight aromatic chains and alkyl groups. The presence of nano fillers seem to have enhanced the stability of these composites at higher temperatures. The $T_{50\%}$ value of the nanofiller incorporated epoxy samples is significantly enhanced compared to pristine epoxy. Incorporation of 1 wt% CdO-ZnO increased the $T_{50\%}$ of the composite to approximately 17°C compared to pristine epoxy. This enhancement might be due to the barrier effect of nano CdO-ZnO which impeded the volatilization of high molecular weight polymer chains in the matrix. It can be assumed that at high temperatures, the agglomerations of nano fillers are re-oriented inside the matrix uniformly and protects the polymer from further degradation or mass transport [28]. This also results in increased charring which can observed from the % residual $mass_{800}$.

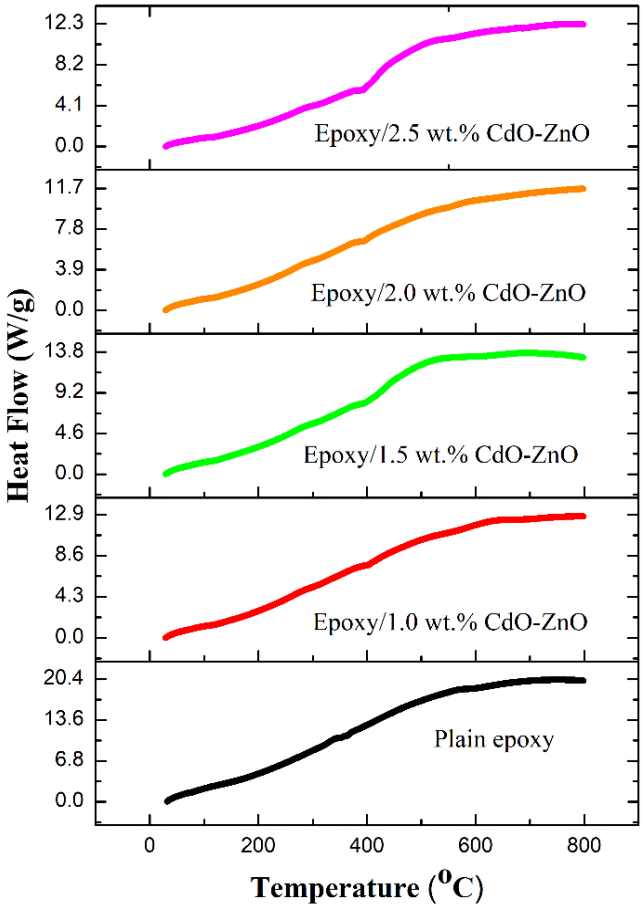

Figure 6(a). DSC of epoxy/CdO-ZnO composites.

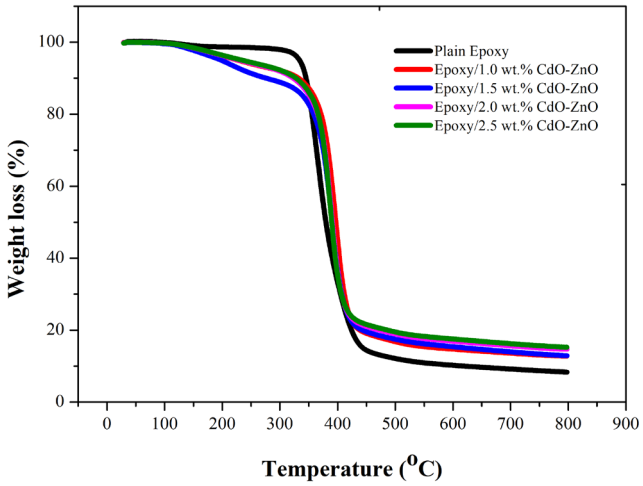

Figure 6(b). TGA of epoxy/CdO-ZnO composites.

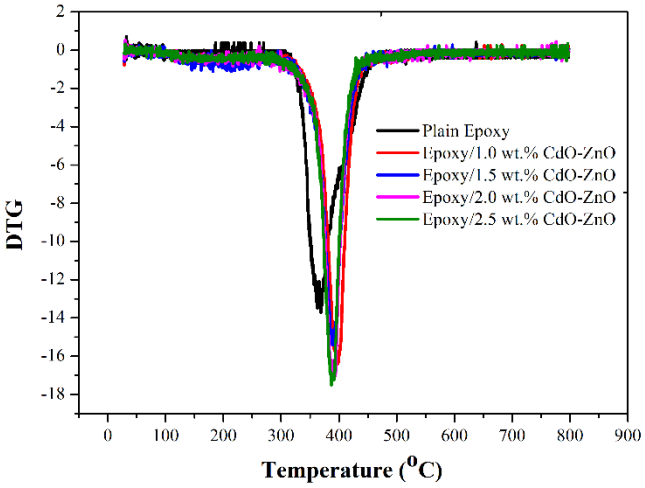

Figure 6(c). DTG thermogram of epoxy/CdO-ZnO composites.

3.5 FTIR spectra

The FTIR spectra of epoxy/CdO-ZnO composites are shown in Figure 7. The presence of ketone groups is indicated in the region between 700 cm^{-1} to 780 cm^{-1} [29]. The peaks obtained in the range of 3390 cm^{-1} to 3450 cm^{-1} indicate the O-H group stretching vibrations [30]. Symmetrical and asymmetrical stretching of CH_3 and CH_2 groups are indicated by the two peaks appearing at 2954 cm^{-1} and 2926 cm^{-1} respectively [30]. The stretching modes of C=C group appear at 1608 cm^{-1} and 1509 cm^{-1} [31]. Epoxide ring vibration was obtained at 1242, 1033, 1032, 1039, and 1008 cm^{-1} peaks [30,31]. The C-H stretching peak corresponding to 1242 cm^{-1} [32].

The peaks obtained at 810 cm^{-1} to 840 cm^{-1} correspond to metal oxide stretching groups, indicate the presence of CdO-ZnO nanoparticles [18]. It is observed that, with increase in addition of CdO-ZnO nanoparticles, the peak obtained in the range of 810 cm^{-1} to 822 cm^{-1} becomes more intense. Various other uneven peaks observed in plain epoxy tends to become prominent and sharper in appearance with filler addition.

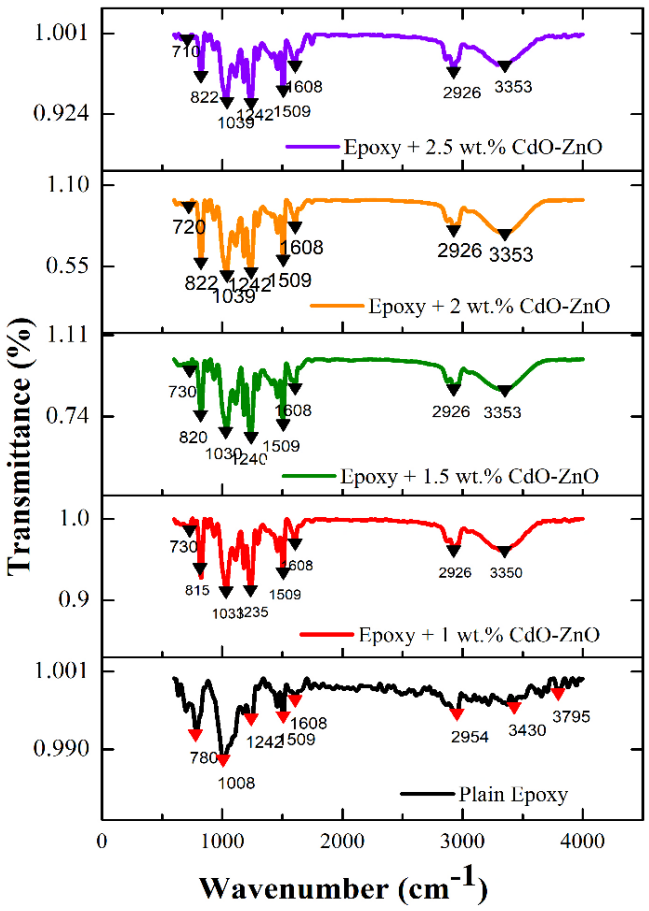

Figure 7. FTIR spectra of epoxy/CdO-ZnO composites.

3.6 Mechanical properties of Epoxy/CdO-ZnO composites

All the mechanical properties of epoxy/CdO-ZnO composites were estimated using standard ASTM procedures. Tensile properties, flexural properties and compressive properties were performed as per ASTM D638, ASTM D790 and ASTM D695 respectively.

3.6.1 Tensile properties

Figure 8 shows the stress-strain relationship of epoxy/CdO-ZnO composites. Plain epoxy is found to exhibit neither the best properties nor inferior properties, it can be said that the plain epoxy has intermediate properties. The highest energy at breakeven point 23.6% is observed for plain epoxy as well as epoxy/1.5 wt% CdO-ZnO. Whereas the toughness, ultimate tensile strength and Young's modulus values were found to be the highest for epoxy/1 wt% CdO-ZnO. This may be due to interaction between the epoxy molecules with CdO-ZnO molecules has led to strong adhesion bonding and hence has a profound impact at that particular concentration itself.

Interfacial phenomenon between the nano fillers and the epoxy matrix plays a vital role in deciding various properties such as toughness, stiffness, transfer of load between the matrix and the reinforcement. In most of the cases the polymer matrix is responsible for deformation of the material. Reinforcing the polymer matrix with nano fillers

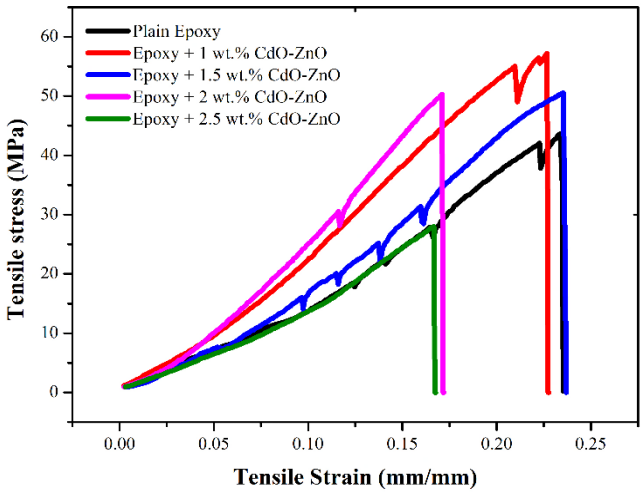

Figure 8. Tensile stress-Tensile strain relationship of epoxy/CdO-ZnO composites.

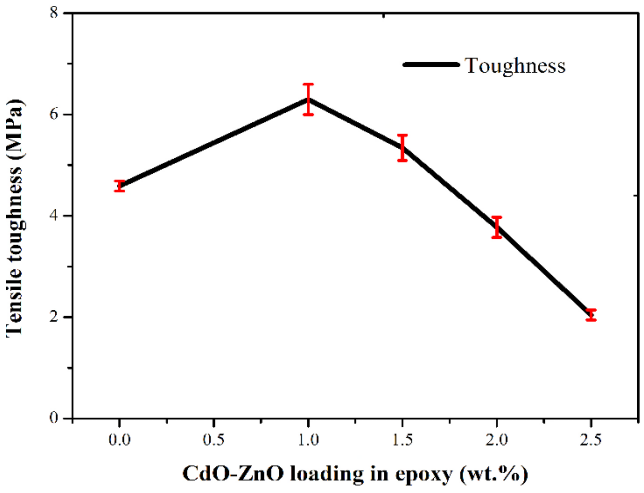

Figure 9. Effect of CdO-ZnO loading on tensile toughness of epoxy composites.

leads to enhanced interaction between the molecules contributing to increase in the ability of the polymer composite to transfer heavy loads, increase in yield strength, stiffness, enhanced modulus values and decrease in the fracture strain. Hence, increase in filler content generally reduces the energy at breakeven point [2,33].

Tensile toughness was calculated by finding out the area under the curve of tensile stress v/s tensile strain graph. Figure 9. shows that with increase in the filler content the tensile toughness increased only for 1 wt% and 1.5 wt.% loading of CdO-ZnO in epoxy then, a gradual decrease with further increase in filler content was observed. It is clear that at low concentration of the filler content, better tensile toughness is achieved due to better bonding and adhesion between the epoxy and nanofiller. High concentrations of the nanofiller in epoxy is found to have detrimental effect on tensile toughness since it is making the polymer composite brittle and consequently reducing the tensile toughness. Other factors such as poor dispersion of filler particles, formation of voids and agglomerates also contribute to decline in tensile toughness at high concentrations of nano filler.

Figure 10 represents the ultimate tensile strength (UTS) of plain epoxy and varying concentrations of epoxy loaded with CdO-ZnO. It is clear that, with increase in the nano filler concentration the ultimate tensile strength increases and almost remains constant at 2 wt% loading of CdO-ZnO in epoxy. Once the concentration increases beyond 2 wt% of CdO-ZnO in epoxy there is a drastic fall in the tensile strength, indicating that it has lost all its tensile properties. The loss in tensile strength may be due to the increase in hardness and brittle nature of the polymer composite.

Young's modulus of all the polymer composites along with epoxy are shown in Figure 11. It can be observed from the graph that, Young's modulus values of all the polymer composites are much higher compared to plain epoxy. Highest value of Young's modulus was observed for epoxy with 1 wt% loading of CdO-ZnO with 277.4MPa, which means that a profound increase of 107.94% in Young's modulus for the polymer composite. This may be due to the effective cross-linking between the polymeric chains of epoxy and nano fillers has resulted in a significant change and enhanced Young's modulus for all the polymer composites.

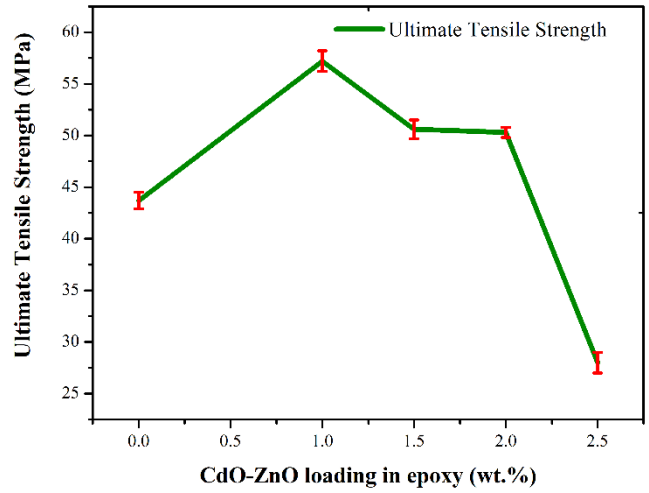

Figure 10. Effect of CdO-ZnO loading on ultimate tensile strength of epoxy composites.

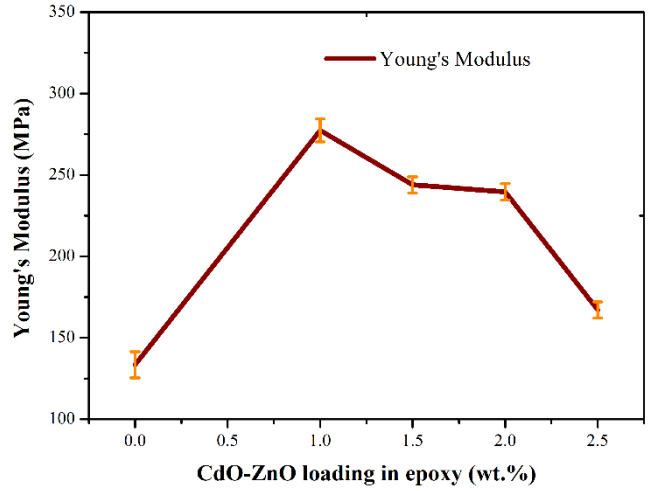

Figure 11. Effect of CdO-ZnO loading on Young's Modulus of epoxy composites.

Table 2 summarises all the tensile properties of the epoxy and varying concentrations of polymer composites. It can be observed that, best results were observed for epoxy/1 wt% CdO-ZnO which

indicates that the polymer composite has good load bearing capacity and better adherence between epoxy and nano particles. The reduction in the strain component has also led to enhanced tensile properties at low concentrations.

The micrographs of tensile fracture surface of epoxy composites are presented in Figure 12(a-e). The tensile fractured surface of plain epoxy (Figure 12(a)) is observed to have a smooth surface consisting of micro-voids and several minute brittle-fractures. The voids/cavities present in the matrix deflect crack propagation to some extent even when the nano-inclusions are absent inside the matrix; however, the deflection or resistance is fairly weak compared to nanofillers incorporated epoxy matrices. The highest mechanical strength was observed for epoxy with 1 wt% CdO-ZnO, which typically means that the nanoparticles are optimally dispersed inside the matrix at that particular concentration. Observing Figure 12(b), clear river-like patterns, also known as hackle markings, can be seen which originate when the crack reaches the threshold speed and dissipates the stored energy in bifurcation [34,35]. This kind of a mechanism is generally observed when the particle-matrix interface is sufficiently strong. In addition to this, various toughening mechanisms have also been observed in the hackle zone. The minute voids which can be observed is due to the particle pull-out toughening (toughening mechanism A) [35-37]. In this case, the voids or nanocavities are formed due to debonding of nanoparticles from the epoxy matrix after fracture. This creates a hump at one side of the fracture and a nanocavity on the other side. The hump resists and deflects crack propagation (toughening mechanism C). Plastic void growth (toughening mechanism B) is also a popular toughening mechanism observed in thermoset polymer composites. Plastic void growth occurs when the nanoparticles are loosely bonded to the base polymer and there is void surrounding the nanoparticles. The crack deflected by the nanoparticle will further deviate due to surrounding void thereby delaying fracture [38]. Contrarily, as the concentration of nanoparticles in the base polymer is increased, there will be a gradual decrease in the mechanical strength. At high nanoparticle concentrations, agglomerations inside the matrix leads to irregular debonding or particle pull-out (Figure 12(d-e)). It also creates an area of high stress concertation which leads to irregular distribution of the applied stress/strain. Eventually, it would lead to the formation of a 'microcomposite' rather than a nanocomposite. Homogeneous dispersion of nanoparticles inside the matrix is a crucial part of toughening mechanism [39].

Table 2. Tensile properties of epoxy/CdO-ZnO polymer composites**.**

CdO-ZnO content (wt%)	Young's modulus (MPa)	%Increase in Young's modulus	Tensile toughness (MPa)	Energy at break point (N)	Ultimate tensile strength (MPa)
0.0*	133.40	-	4.58	23.60	43.70
1.0	277.40	107.94	6.29	22.67	57.20
1.5	243.90	82.83	5.34	23.60	50.60
2.0	239.60	79.61	3.77	17.10	50.30
2.5	167.10	25.26	2.04	16.67	28.00

*refers to plain epoxy.

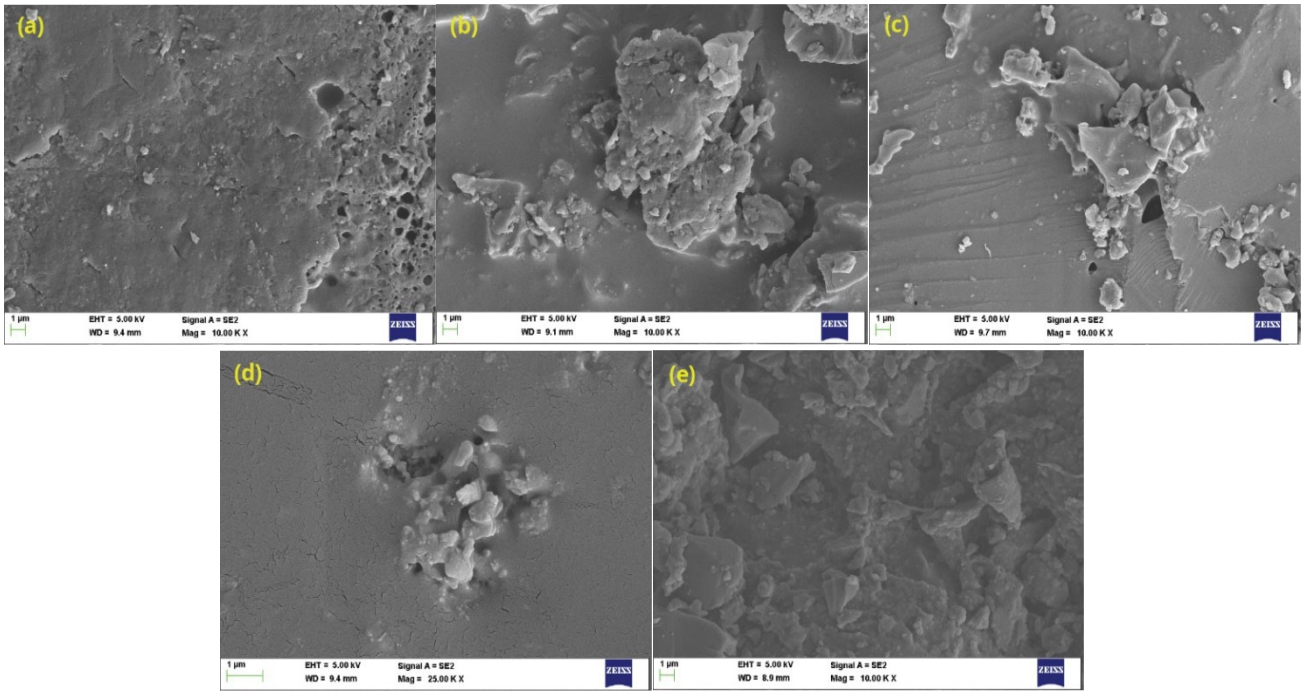

Figure 12. SEM micrographs of tensile-fractured surface of (a) plain epoxy, (b) epoxy/1.0 wt% CdO-ZnO, (c) epoxy/1.5 wt% CdO-ZnO, (d) epoxy/2.0 wt% CdO-ZnO, and (e) epoxy/2.5 wt% CdO-ZnO.

3.6.2 Flexural properties

Flexural properties such as flexural strength, flexural modulus and flexural toughness were analysed and reported. Graph indicating the flexural stress vs flexural strain for epoxy polymer nanocomposite are shown in Figure 13. It is clear from the figure that lowest and highest flexural strain was observed in epoxy/2 wt% CdO-ZnO respectively. Highest flexural strain also indicates highest energy at breakeven point which was found to be 4.68%. Further addition of nano filler resulted in decrease in the strain component and breakeven points. All the flexural properties reached a maximum at epoxy/1 wt% CdO-ZnO, with further increase in nano filler concentration, decrease in flexural properties was observed.

Flexural strength epoxy/CdO-ZnO composites are shown in Figure 14. Increase in the nano filler loading has contributed to increase in the flexural strength of all the composites. Even though the values seemed to be more than double for epoxy/1 wt% CdO-ZnO loading as compared to plain epoxy, however a steep decline was observed with further incorporation of CdO-ZnO nanoparticles. The highest value of flexural strength of 5.9 MPa was observed for epoxy/1 wt% CdO-ZnO composite.

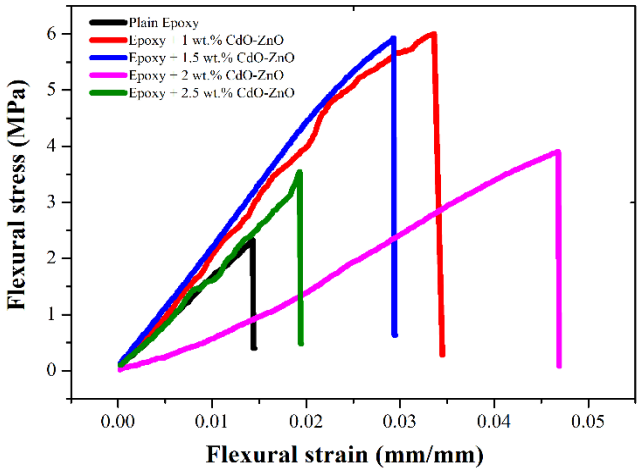

Figure 13. Flexural Stress- Flexural Strain relationship of epoxy/CdO-ZnO composites.

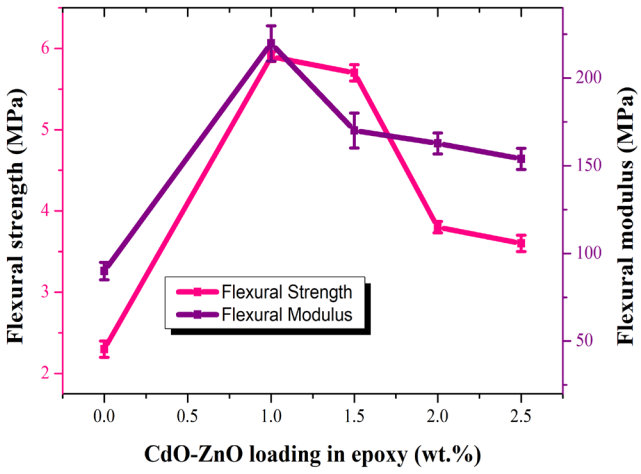

Figure 14. Effect of CdO-ZnO loading on flexural strength and flexural modulus of epoxy composites.

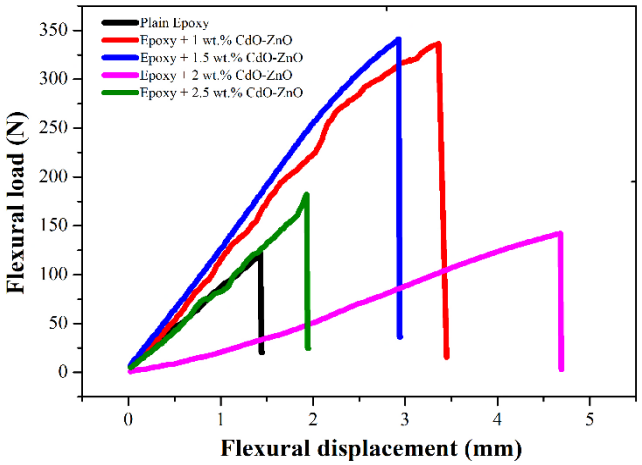

Figure 15. Flexural load vs displacement relationship of epoxy and for varying concentrations of CdO-ZnO nanoparticles.

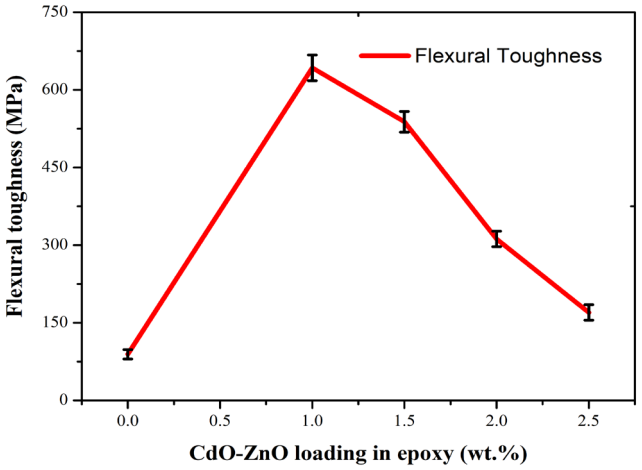

Figure 16. Effect of CdO-ZnO loading on flexural toughness of epoxy composites.

Figure 14 also indicates the effect of nano filler loading on flexural modulus of epoxy composites. A steep increase in flexural modulus value was observed with just 1 wt% loading of CdO-ZnO nanoparticles in epoxy. Further addition of CdO-ZnO nanoparticles in epoxy showed a steep decrease in flexural modulus values. Highest flexural modulus of 219.7 MPa was observed for epoxy/1 wt% CdO-ZnO composite, which indicated that there was a profound increase of 144.38% in flexural modulus as compared with plain epoxy.

Another important mechanical property called the flexural toughness was calculated using area under the curve of flexural load vs flexural displacement [40] are indicated in Figure 15. It is evident from the figure that least load vs displacement was observed for plain epoxy, which means that plain epoxy exhibited least flexural toughness and can undergo deformation even when loads as low as 120 N is applied. This phenomenon occurs when the polymer is unable to transfer loads. The highest area under the curve was observed for epoxy/1 wt% CdO-ZnO composite. However, highest flexural displacement at low load was observed for epoxy with 2 wt% nanofiller. Overall, we can say that incorporation of CdO-ZnO into epoxy has built up a strong bond and excellent interaction between the polymer molecules and the nano filler which acts as a reinforcing

agent and hence, it has given the ability to totally transform the polymer composite as a whole by building up resistance against deformation at higher loads as compared to plain epoxy.

Figure 16 shows the effect of nanofiller loading on flexural toughness values of epoxy composites. Incorporation of CdO-ZnO as nanofiller has a linear relationship with flexural toughness. As seen from the graph, the flexural toughness of plain epoxy was 89.31 MPa and for epoxy/1 wt% CdO-ZnO nanoparticles the flexural toughness was 642.5 MPa, which means that there is a substantial increase of 619.4% in the toughness value when compared with plain epoxy. This is probably due to highest area under the curve for flexural vs flexural displacement. The significance of the area under the flexural load vs flexural displacement curve can be explained as follows; the amount of energy required for the first crack to appear when an ultimate load is applied due to which a deflection occurs in a material and the energy required for the crack to propagate further is explained by the load vs displacement curve [40]. By this, we can say that highest amount of energy was required for epoxy with 1 wt% CdO-ZnO loading for an initial crack to appear for an ultimate load of 336 N and for the crack to propagate further, finally resulting in a deflection to occur. Hence, 336 N is the cracking load for epoxy with 1 wt% loading of CdO-ZnO nanoparticles [40]. Table 3 summarises all the flexural properties of the epoxy and varying concentrations of polymer composites.

3.6.3 Compressive properties

Compressive properties such as compression modulus, compressive strength and compressive toughness were analysed for epoxy/CdO-ZnO composites. Compressive stress v/s compressive strain relationship for the polymer composites are shown in Figure 17. It is clear from the graph that, with increase in the nano filler concentration in epoxy, all the compressive properties begin to enhance and the highest compressive strength, compression modulus and compressive toughness is exhibited by epoxy/1 wt% CdO-ZnO nanoparticles, with further increase in the nano filler concentration in epoxy, all the compressive properties begin to decline. Hence increase in nanofiller concentration beyond 1 wt% concentration in epoxy was found to have detrimental effect on compressive properties.

Effect of nano filler concentration on compressive strength are shown in Figure 18. Initially with increase in CdO-ZnO concentration, the compressive strength of polymer composites began to increase. Even though the increase was not very significant and it was as low as 6.8%, this slight increase in compressive strength may have been contributed due to good adhesion between the nano particles and the epoxy matrix owing to improved interfacial interaction between molecules. Increase in concentration of CdO-ZnO nanoparticles beyond 1 wt% concentration has led to drastic fall in the compressive strength of the polymer composites. Three main reasons might have contributed to such a premature failure of the polymer composites. Firstly, increase in CdO-ZnO concentration might have reduced the reactive sites present in the composite leading to saturation of the nanofiller and hence the development of agglomeration of the molecules. These agglomerated molecules fail to resist compressive loads applied on the polymer composite [41]. Secondly, the localised stress that is created when compressive loads are applied might result in formation of inter platelets. These inter platelets slide over each other resulting in premature failure at high loading of nano filler [42]. Lastly, the plastic strain and elastic-plastic modulus play a vital role in deciding the compressive load bearing capacity of a polymer composite. When the plastic strain and elastic-plastic modulus of plain epoxy becomes higher compared to the polymer composites, the compressive strength eventually reduces [42].

Figure 18 shows the influence of CdO-ZnO molecules on compression modulus of epoxy composites. Incorporation of nano filler in epoxy has led to a steep increase in the compression modulus values. The compression modulus values for plain epoxy was found to be 7626 MPa whereas, for epoxy with 1 wt% concentration of CdO-ZnO nanoparticles was found to be 9745.8 MPa. This significant rise in modulus values may be due to the steeper slope observed in the elastic region for 1 wt% and 1.5 wt% CdO-ZnO in epoxy in the compressive stress vs compressive strain curve. The reduction of modulus values for the polymer composites beyond 1 wt% concentration of CdO-ZnO in epoxy may have arisen due to the formation of localised stresses under compression [42,43]. This results in weakening of the interfacial adhesion between the molecules of the epoxy and nano filler. Some of the researches report similar results on decrease of compressive strength and compression modulus on increase in nano filler concentration [42,43].

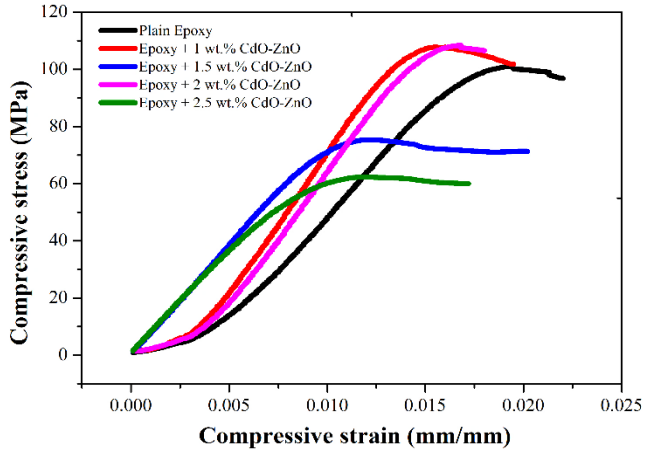

Figure 17. Compressive Stress v/s Compressive Strain relationship of epoxy and for varying concentrations of CdO-ZnO in epoxy.

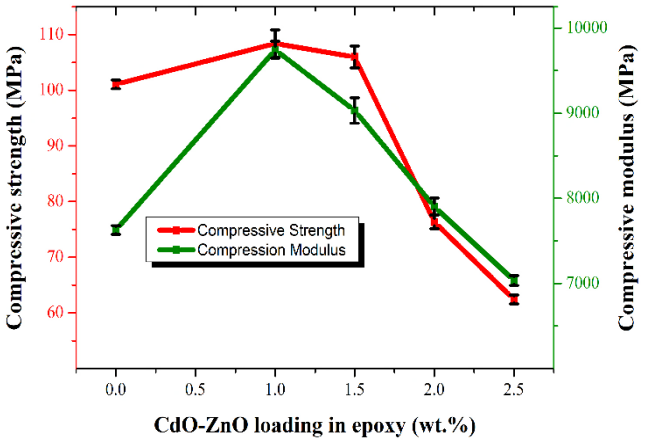

Figure 18. Effect of CdO-ZnO loading on compressive strength and compressive modulus of epoxy composites.

Table 3. Flexural properties of epoxy/CdO-ZnO composites.

CdO-ZnO content (wt%)	Flexural modulus (MPa)	% Increase in flexural modulus	Flexural toughness (MPa)	% Increase in flexural toughness	Flexural strength (MPa)	% Increase in flexural strength
0.0*	89.90	-	89.31	-	2.30	-
1.0	219.70	144.38	642.50	619.40	5.90	156.51
1.5	170.00	89.09	538.40	502.84	5.80	152.17
2.0	162.70	80.97	312.00	249.34	3.80	65.21
2.5	153.90	71.19	170.00	90.34	3.60	56.52

*refers to plain epoxy.

Table 4. Effect of CdO-ZnO content on compression properties of epoxy composites.

CdO-ZnO content (wt%)	Compression modulus (MPa)	Compressive toughness (MPa)	Compressive strength (MPa)
0.0*	7626.00	0.98	101.10
1.0	9745.80	1.19	108.40
1.5	9032.50	1.11	106.00
2.0	7902.00	0.98	76.30
2.5	7034.00	0.78	62.40

*refers to plain epoxy

3.7 Electrical properties

Electrical properties such as impedance spectroscopy, dielectric permittivity, electrical modulus and electrical conductivity were analysed and reported for epoxy/CdO-ZnO composites.

Figure 19 represents the role of nano filler on toughness of the epoxy/CdO-ZnO composites. Initially as observed from the figure, an increase of 21% in the toughness values were observed when the epoxy was loaded with 1 wt% concentration of CdO-ZnO nano-particles as compared to plain epoxy. The reduction in toughness values with further increase in the nano filler concentration was due to the transformation of the epoxy to a brittle material which further led to deformation the polymer composite at lower compressive loads [42,43]. This indicated that higher loadings of nano filler had detrimental effect on compressive toughness of the epoxy polymer composites. Table 4 summarises all the compressive properties of the epoxy and varying concentrations of polymer composites.

3.7.1 Impedance spectroscopy analysis

Impedance spectroscopy analysis was used to investigate the electrical properties of epoxy/CdO-ZnO composites. Complex impedance (Z*) can best explained by Debye model as shown in Equation (2) [44]:

$$Z^* = Z' + iZ'' = R/(1+i\omega\tau) \quad (2)$$

Where Z′ is the real part of complex impedance as shown in Equation (3) [44] and Z″ is the imaginary part of complex impedance as shown in Equation (4) [44] and τ is the relaxation time as shown in Equation (5) [44] and ω is the angular frequency.

$$Z' = R/[1+i(\omega RC)^2] \quad (3)$$

$$Z'' = \omega R^2 C/[1+(\omega RC)^2] \quad (4)$$

$$\tau = RC \quad (5)$$

Figure 20 depicts the variation of real part of complex impedance (Z′) with frequency. It is evident that Z′ is found to decrease with increase in frequency, which indicates an increase in conductivity with increase in frequency [44]. The Z′ values of all the composites are found to merge at certain frequency and then remain constant thereafter. This phenomenon occurs due to decrease in the barrier properties that occurs at high frequencies which leads to the release of space charge in the composites. The typical dip that occurs just before all the Z′ values of composites merge at high frequencies is called as charge carrier hopping [44].

Figure 21 shows the variation of imaginary part of complex impedance (Z″) with frequency. A typical dip Z″ is observed with increase in frequency, this dip is mainly caused due to charge carrier hopping effect. At very high frequencies sharp, prominent peaks were observed for all the epoxy composites. This significant increase in peak height at high frequencies is called as relaxation frequency (f_{max}). Since Z″ peak shift was observed at very high frequency, consequently the relaxation time began to decrease steeply, as relaxation time and f_{max} share an inverse relationship as shown in Equation (6) [44]:

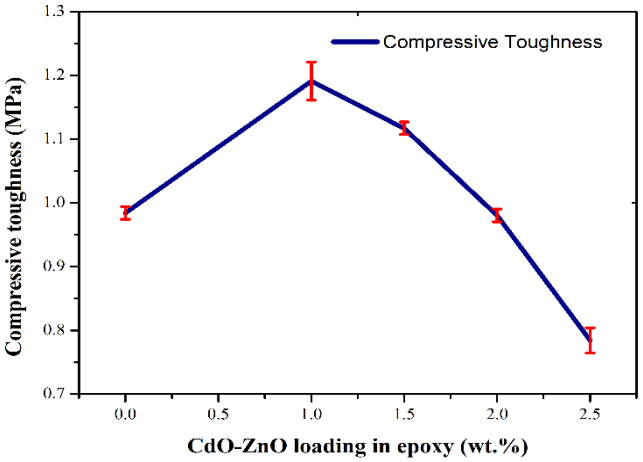

Figure 19. Effect of CdO-ZnO loading on compressive toughness of epoxy composites.

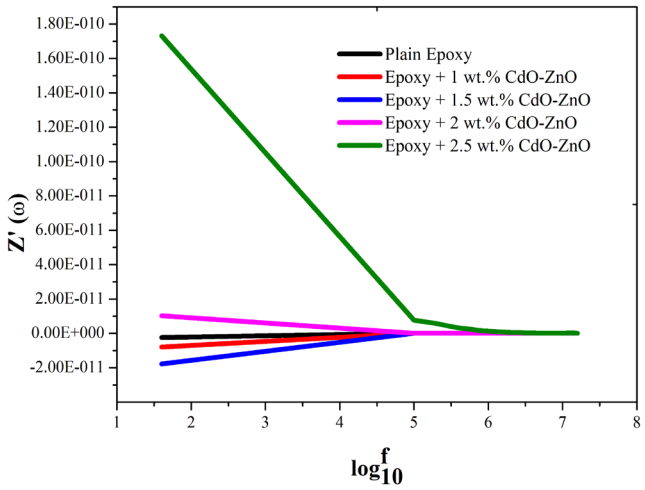

Figure 20. Z′ vs log^{f} for epoxy/CdO-ZnO composites.

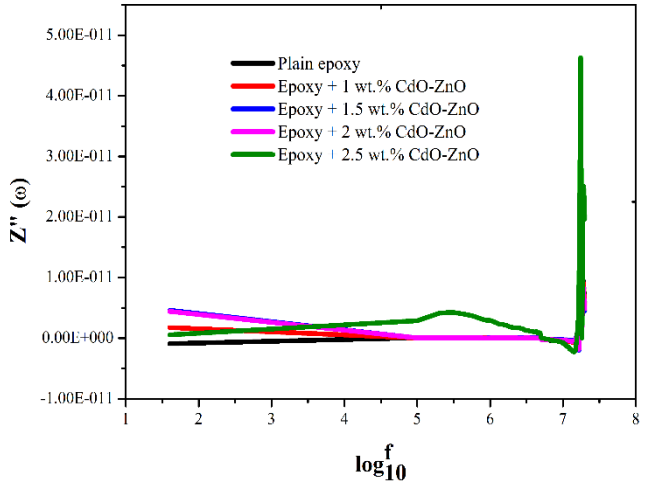

Figure 21. Z″ vs log^{f} for epoxy/CdO-ZnO composites.

$$\tau = 1/2\Pi f_{max} \quad (6)$$

Z″ peak shift occurred mainly due to three reasons namely; hopping of electrons, space charge relaxation and space charge polarization at high frequencies due to oxygen vacancies and grain boundaries present in the epoxy composites.

3.7.2 Dielectric permittivity analysis

The two key important frequency dependent dielectric parameters; dielectric constant (ε') and dielectric loss (ε'') were analysed and reported. The variation of dielectric constant with frequency for epoxy/CdO-ZnO composites are shown in Figure 22. At low frequencies high dielectric constant values are observed for epoxy and epoxy composites, this is probably due to interfacial polarization or Maxwell-Wagner type of polarization occurring in the epoxy composite which also leads to electrode effect to occur [18]. The grain boundaries present in the epoxy composites act as carriers to induce space charges that act as dipoles which result in polarization to occur. Lower the frequency, higher the effectiveness of the grain boundary in epoxy composites [44]. Hence, dielectric constant values tend to be high at low frequencies. Gradual decrease in dielectric constant value is observed with increase in frequency this is because, for an applied electric field the dipoles tend to orient themselves. At very high frequencies, a sudden increase in the dielectric constant values is observed, this may be probably due to the reason that the dipolar groups are finding difficulty in orienting themselves at very high frequencies [18]. This shows that, epoxy/CdO-ZnO composites behave like a semiconducting material.

Dielectric loss of epoxy/CdO-ZnO composites are shown in Figure 23. From the figure it is evident that, a gradual decrease in dielectric loss with increase in frequency is observed. This is because, at low frequencies the dipoles get sufficient time for orientation. Dielectric loss is found to decrease with increase in frequency. This might be due to the fact that the dipoles have insufficient time to orient themselves to applied electric field and also to reorient themselves for change in the direction of applied electric field [44]. The decrease in dielectric loss with increase in frequency also indicates minimum heat losses [45]. Hence, heat is not generated at very high frequencies.

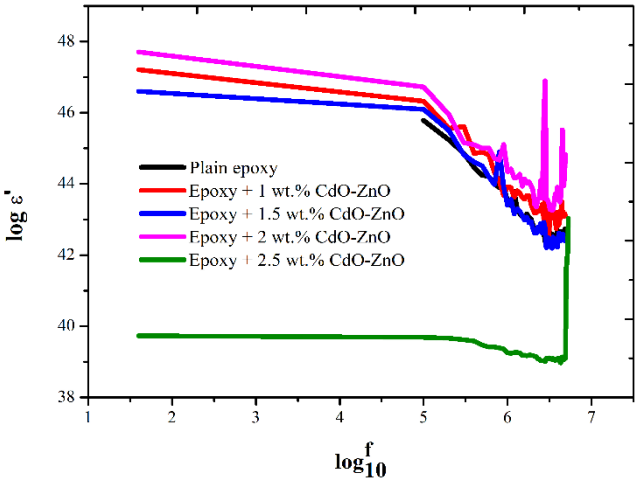

Figure 22. ε' vs log^{f} for epoxy/CdO-ZnO composites.

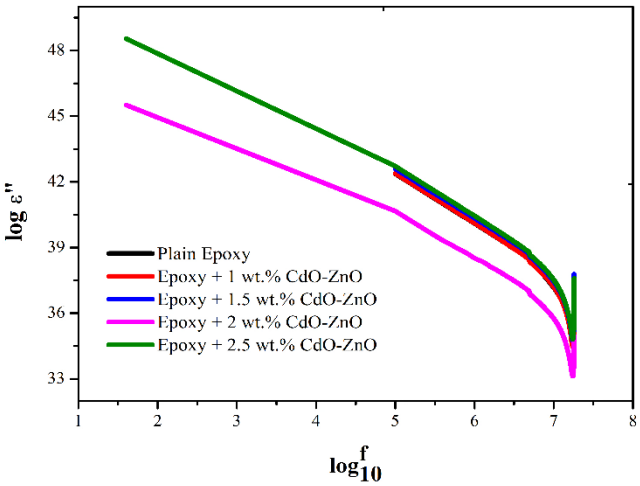

Figure 23. ε'' vs log^{f} for epoxy/CdO-ZnO composites.

3.7.3 Electrical modulus spectrum analysis

Electrical modulus spectroscopy is used to understand the dielectric relaxation behaviour of epoxy composites. Electrical modulus studies

are used to analyse the transport mechanism of charge carriers, conductivity relaxation and ionic polarization occurring within the composites when subjected to different frequencies. Complex electrical modulus can be represented by Equation (7) [44]:

$$M^* = M' + jM'' = j\omega C_o Z^* \quad (7)$$

The real part of complex electrical modulus can be represented as shown in Equation (8) [44]:

$$M' = \omega C_o Z'' \quad (8)$$

The imaginary part of complex electrical modulus can be represented as shown in Equation (9) [44]:

$$M'' = \omega C_o Z' \quad (9)$$

Capacitance in free space (C_o) is represented by Equation (10) [44]:

$$C_o = \varepsilon_o A/t \quad (10)$$

Where; ε_o = permittivity of free space
A = area of the electrode
t = sample thickness.

Figure 24 shows the variation of real part of complex electrical modulus with frequency for epoxy/CdO-ZnO composites. At low frequencies, M′ values tend to be almost zero, this is due to ionic polarization existing within the composites. As there is an increase in frequency linear increase in M′ value is observed. This is mainly attributed due to the mobility of charge carriers at high frequency. A sudden decrease in value is observed at very high frequency this is probably due to the hopping of electrons, space charge relaxation and grain boundaries present in the epoxy composites. The large difference in electrical properties for 2.5 wt% CdO-ZnO/epoxy composites as compared to other concentrations is observed due to the fact that epoxy is completely saturated with nanofiller, blocking most of the epoxy reactive sites resulting in formation of voids and agglomerates [45,46].

The frequency response of the imaginary part of electrical modulus (M″) are shown in Figure 25. At low frequency, very low values of M″ is observed. This is because, the ions are free to move in the composite and hopping from one site to another is possible. As the frequency keeps on increasing, peak shift occurs. Three prominent maxima peaks are observed at very high frequencies; these maxima peaks indicate localised motion of the charge carriers within the epoxy composites that are spatially confined in their own potential wells [44]. These maxima peaks also indicate the presence of grain boundary within the epoxy composites.

3.7.4 Electrical conductivity analysis

Electrical conductivity measurements for epoxy composites were made using Equation 11 [44]:

$$\sigma_{ac} = t/\ Z'A \quad (11)$$

Frequency dependence of AC electrical conductivity for epoxy/CdO-ZnO composites are shown in Figure 26.

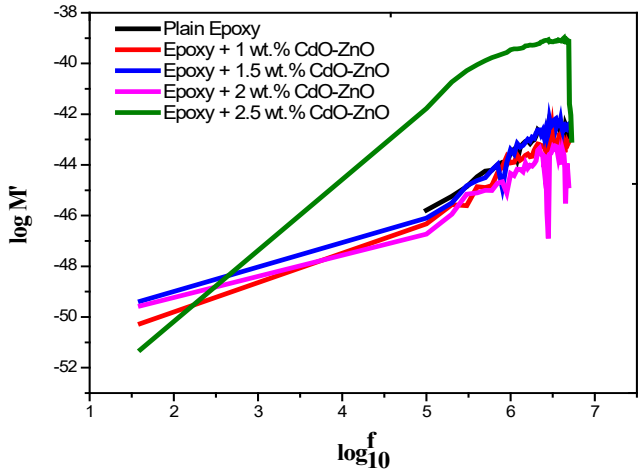

Figure 24. M′ vs log^f for epoxy/CdO-ZnO composites.\

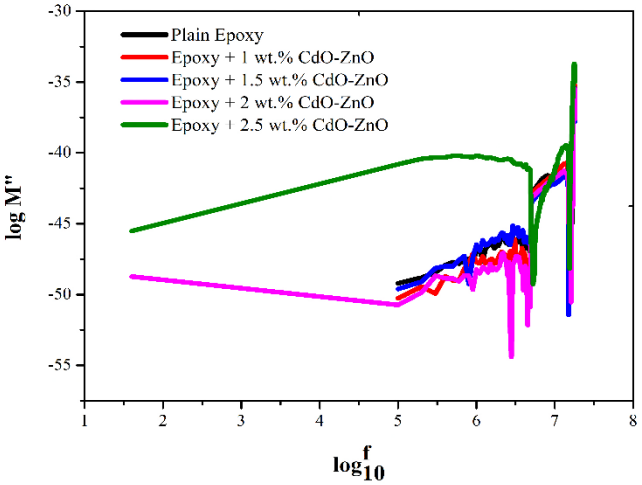

Figure 25. M″ vs log^f for epoxy/CdO-ZnO composites.

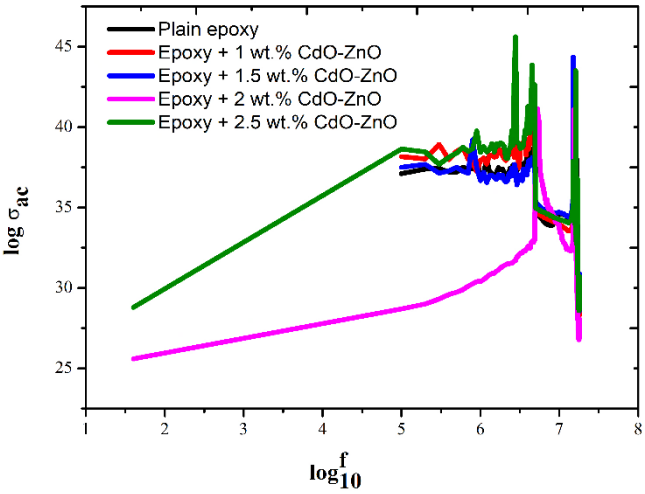

Figure 26. Variation of AC electrical conductivity with frequency for epoxy/CdO-ZnO composites.

4. Conclusion

CdO-ZnO was doped into epoxy and casted using moulds. The nanopowder and epoxy composites were characterized for its structural properties using SEM, XRD and FTIR spectra. The SEM results showed uniform distribution of porous nanoparticles. XRD graphs revealed well defined sharp crystalline peaks. FTIR spectra showed enhanced interaction of nanoparticles with the matrix. UV-Vis spectra showed enhanced UV-Shielding capacity of the epoxy composites. DSC, TGA and DTG results showed enhanced stability of epoxy composites at higher temperatures. The polymer composites were tested for mechanical properties such as tensile properties, flexural properties and compression properties using Zwick UTM. Best tensile properties for the polymer composites were obtained for 1 wt% CdO-ZnO in epoxy with a significant increase of 107.94% increase in the Young's modulus values. Excellent flexural properties were observed for 1 wt% CdO-ZnO in epoxy with a drastic increase of 144.38% in the flexural modulus values and substantial increase of 619.4% in the flexural toughness value was observed due to the good load bearing capacity and better adherence among the epoxy and nano fillers. Good enhancement among all the compression properties were observed for 1 wt% CdO-ZnO in epoxy. Hence we can conclude stating that, the polymer composites synthesized with 1 wt% concentration of CdO-ZnO in epoxy enhanced the tensile properties, flexural properties and compression properties. Electrical properties such as electrical impedance, dielectric permittivity, electrical modulus and AC electrical conductivity were estimated. The electrical results revealed that, the composites exhibit a typical semiconducting behaviour at high frequencies. These composites can be promising materials for mechanical and semiconducting applications.

Acknowledgements

The authors are very grateful to Department of Science and Technology, for providing financial assistance under Women Scientist A-Scheme to carry out the entire project. Project Sanction No. SR/ WOS-A/ET-16/2017. They are also thankful to Department of Chemical Engineering, MSRIT, Bangalore, for the technical support to carry out the research work and Centre for Advanced Materials Technology of MSRIT Bangalore for providing facility for research work. Mechanical testing was performed at TERI, Bangalore. SEM, EDX, UV-VIS DRS, and electrical properties were tested at CeNSE lab, IISC, Bangalore.

References

1. G. K. Mahadeva Raju, C. Srikanth, G. M. Madhu, D. P. Shankar Reddy, and K. V. Karthik, "Fly ash epoxy composites with superior fire retardant properties," In *Advanced Materials Research,* vol. 1172, pp. 83-94, 2022.
2. B. Wetzel, F. Haupert, and M. Q. Zhang, "Epoxy nanocomposites with high mechanical and tribological performance," *Composites Science and Technology,* vol. 63, pp. 2055-2067, 2003.
3. R. Walter, K. Friedrich, V. Privalko, and A. Savadori, "On modulus and fracture toughness of rigid particulate filled high density polyethylene," *The Journal of Adhesion,* vol. 64, pp. 87-109, 1997.
4. M. F. Hochella Jr, "Nanoscience and technology: The next revolution in the Earth sciences," *Earth and Planetary Science Letters,* vol. 203 pp. 593-605, 2002.
5. B. Wetzel, F. Haupert, K. Friedrich, M. Q. Zhang, and M. Z. Rong, "Impact and wear resistance of polymer nanocomposites at low filler content," *Polymer Engineering & Science,* vol. 42 pp. 1919-1927, 2002.
6. R. M. Laine, J. Choi, and I. Lee, "Organic–inorganic nano-composites with completely defined interfacial interactions," *Advanced Materials,* vol. 13, pp. 800-803, 2001.
7. Q. Wang, Q. Xue, W. Shen, and J. Zhang, "The friction and wear properties of nanometer ZrO_2-filled polyether-etherketone," *Journal of applied polymer science,* vol. 69, pp. 135-141, 1998.
8. C. B. Ng, L. S. Schadler, and R. W. Siegel, "Synthesis and mechanical properties of TiO_2-epoxy nanocomposites," *Nanostructured materials,* vol. 12, pp. 507-510, 1999.
9. M. Q. Zhang, M. Z. Rong, S. L. Yu, B. Wetzel, and K. Friedrich, "Improvement of tribological performance of epoxy by the addition of irradiation grafted nano-inorganic particles," *Macromolecular materials and engineering*, vol. 287, pp. 111-115, 2002.
10. Q. Wang, Q. Xue, and W. Shen, "The friction and wear properties of nanometre SiO_2 filled polyetheretherketone," *Tribology International,* vol. 30, pp. 193-197, 1997.
11. C. Srikanth, and G.M. Madhu, "Effect of ZTA concentration on structural, thermal, mechanical and dielectric behavior of novel ZTA–PVA nanocomposite films," *SN Applied Sciences,* vol. 2, pp. 1-12, 2020.
12. Y. Luo, M. Z. Rong, and M. Q. Zhang, "Covalently connecting nanoparticles with epoxy matrix and its effect on the improvement of tribological performance of the composites," *Polymers and Polymer Composites*, vol. 13, pp. 245-252, 2005.
13. M. Avella, M. E. Errico, S. Martelli, and E. Martuscelli, "Preparation methodologies of polymer matrix nanocomposites," *Applied organometallic chemistry,* vol. 15, pp. 435-439, 2001.
14. Q. I. Wang, H. Xia, and C. Zhang, "Preparation of polymer/ inorganic nanoparticles composites through ultrasonic irradiation," *Journal of applied polymer science,* vol. 80, pp. 1478-1488, 2001.
15. C. Srikanth, G. M. Madhu, and S. J. Kashyap, "Enhanced structural, thermal, mechanical and electrical properties of nano ZTA/epoxy composites," *AIMS Materials Science,* vol. 9, pp. 214-235, 2022.
16. J. Sanes, F. J. Carrión, and M. D. Bermúdez, "Effect of the addition of room temperature ionic liquid and ZnO nano-particles on the wear and scratch resistance of epoxy resin," *Wear,* vol. 268, pp. 1295-1302, 2010.
17. K. H. Ding, G. L. Wang, and M. Zhang, "Characterization of mechanical properties of epoxy resin reinforced with submicron-sized ZnO prepared via in situ synthesis method," *Materials & Design*, vol. 32, pp. 3986-3991, 2011.
18. C. Srikanth, G. M. Madhu, H. Bhamidipati, and S. Srinivas "The effect of CdO–ZnO nanoparticles addition on structural,

electrical and mechanical properties of PVA films," *AIMS Materials Science,* vol. 6, pp. 1107-1123, 2019.

19. J. S. Sagar, S. J. Kashyap, G. M. Madhu, and P. Dixit, "Investigation of mechanical, thermal and electrical parameters of gel combustion-derived cubic zirconia/epoxy resin composites for high-voltage insulation," *Cerâmica* vol.66, pp.186-196, 2020.
20. M. W. Ho, C. K. Lam, K. T. Lau, D. H. Ng, and D. Hui, "Mechanical properties of epoxy-based composites using nanoclays," *Composite structures,* vol. 75, pp. 415-421, 2006.
21. Y. Q. Li, S. Y. Fu, and Y. W. Mai "Preparation and characterization of transparent ZnO/epoxy nanocomposites with high-UV shielding efficiency," *Polymer,* vol. 47, pp. 2127-2132, 2006.
22. F. M. Uhl, S. P. Davuluri, S. C. Wong, and D. C. Webster, "Organically modified montmorillonites in UV curable urethane acrylate films," *Polymer*, vol. 45, pp. 6175-6187, 2004.
23. T. A. Nguyen, T. V. Nguyen, H. Thai, and X. Shi, "Effect of nanoparticles on the thermal and mechanical properties of epoxy coatings," *Journal of Nanoscience and Nanotechnology,* vol. 16, pp. 9874-9881, 2016.
24. M. Baiquni, B. Soegijono, and A. N. Hakim, "Thermal and mechanical properties of hybrid organoclay/rockwool fiber reinforced epoxy composites," *In Journal of Physics: Conference Series,* vol. 1191, pp. 1-6, 2019.
25. X. Zhang, O. Alloul, Q. He, J. Zhu, M. J. Verde, Y. Li, and Z. Guo, "Strengthened magnetic epoxy nanocomposites with protruding nanoparticles on the graphene nanosheets," *Polymer*, vol. 54, pp. 3594-3604, 2013.
26. S. Sand Chee, and M. Jawaid , The effect of Bi-functionalized MMT on morphology, thermal stability, dynamic mechanical, and tensile properties of epoxy/organoclay nanocomposites," *Polymers*, vol.11, pp. 2012, 2019.
27. D. Bikiaris, "Can nanoparticles really enhance thermal stability of polymers? Part II: An overview on thermal decomposition of polycondensation polymers," *Thermochimica Acta,* vol. 523, pp. 25-45, 2011.
28. Y. Xue, M. Shen, S. Zeng, W. Zhang, L. Hao, L. Yang, and P. Song, "A novel strategy for enhancing the flame resistance, dynamic mechanical and the thermal degradation properties of epoxy nanocomposites," *Materials Research Express,* vol. 6, pp. 125003, 2019.
29. J. E. Katon, and F. F. Bentley (1963) "New spectra-structure correlations of ketones in the 700-750 cm^{-1} region," *Spectrochimica Acta*, vol. 19, pp. 639-653, 1963.
30. D. K. Shukla, S. V. Kasisomayajula, and V. Parameswaran, "Epoxy composites using functionalized alumina platelets as reinforcements," *Composites Science and Technology,* vol. 68, pp. 3055-3063, 2008.
31. M. Abbate, E. Martuscelli, P. Musto, G. Ragosta, and G. Scarinzi, "Toughening of a highly cross-linked epoxy resin by reactive blending with bisphenol A polycarbonate," *Journal of Polymer Science Part B: Polymer Physics,* vol. 32, pp. 395-408, 1994.
32. X. Wang, Y. Hu, L. Song, W. Xing, H. Lu, P. Lv, and G. Jie, "Flame retardancy and thermal degradation mechanism of epoxy resin composites based on a DOPO substituted organo-phosphorus oligomer," *Polymer*, vol. 51, pp. 2435-2445, 2010.
33. C. L. Wu, M. Q. Zhang, M. Z. Rong, and K. Friedrich, "Tensile performance improvement of low nanoparticles filled-polypropylene composites," *Composites science and technology*, vol. 62, pp. 1327-1340, 2002.
34. M. S. Goyat, S. Rana, S. Halder, and P. K. Ghosh, "Facile fabrication of epoxy-TiO_2 nanocomposites: A critical analysis of TiO_2 impact on mechanical properties and toughening mechanisms," *Ultrasonics Sonochemistry,* vol. 40, pp. 861-873, 2018.
35. E. Greenhalgh, *Failure Analysis and Fractography of Polymer Composites*, Woodhead, 2009.
36. B. B. Johnsen, A. J. Kinloch, and A. C. Taylor, "Toughness of syndiotactic polystyrene/epoxy polymer blends: microstructure and toughening mechanisms," *Polymer,* vol. 46, pp. 7352-7369, 2005.
37. S. Zhao, L. S. Schadler, R. Duncan, H. Hillborg, and T. Auletta, "Mechanisms leading to improved mechanical performance in nanoscale alumina filled epoxy," *Composites Science and Technology,* vol. 68, pp. 2965-2975, 2008.
38. B. B. Johnsen, A. J. Kinloch, R. D. Mohammed, A. C. Taylor, and S. Sprenger, "Toughening mechanisms of nanoparticle-modified epoxy polymers," *Polymer,* vol. 48, pp. 530-541, 2007.
39. A. Kumar, K. Kumar, P. K. Ghosh, and K. L. Yadav, "MWCNT/TiO_2 hybrid nano filler toward high-performance epoxy composite," *Ultrasonics sonochemistry*, vol. 41, pp. 37-46, 2018.
40. D. O. Al-Ghamdy, J. K. Wight, and E. Tons, "Flexural toughness of steel fiber reinforced concrete," *Engineering Sciences,* vol. 6, pp. 81-97, 1994.
41. A. Ashamol, V. S. Priyambika , G. S. Avadhani, and R. R. N. Sailaja, "Nanocomposites of crosslinked starch phthalate and silane modified nanoclay: Study of mechanical, thermal, morphological, and biodegradable characteristics," *Starch-Stärke,* vol. 65, pp. 443-452, 2013.
42. A. Jumahat, C. Soutis, J. Mahmud, and N. Ahmad, "Compressive properties of nanoclay/epoxy nanocomposites," *Procedia Engineering,* vol. 41, pp. 1607-1613, 2012.
43. A. K. Subramaniyan, and C. T. Sun, "Enhancing compressive strength of unidirectional polymeric composites using nanoclay," *Composites Part A: Applied Science and Manufacturing,* vol. 37, pp. 2257-2268, 2006.
44. M. A. Rahman, and A. A. Hossain, "Electrical transport properties of Mn–Ni–Zn ferrite using complex impedance spectroscopy," *Physica Scripta,* vol. 89, pp. 025803, 2014.
45. J. K. Rao, A. Raizada, D. Ganguly, M. M. Mankad, S. V. Satayanarayana, and G. M. Madhu, "Investigation of structural and electrical properties of novel CuO–PVA nanocomposite films," *Journal of materials science,* vol. 50, pp. 7064-7074, 2015.
46. S. H. Rashmi, A. Soumyashree, S. Shrusti, S. Shivani, D. Aamir, A. A. Kittur, H. K. Sudhina, J. Koteswararao, and G. M. Madhu, "Structural mechanical and electrical property evaluation of nano cadmium oxide polyvinyl alcohol composites," *International Journal of Plastics Technology*, vol. *22*, pp.41-55, 2018.